PCCP

Conditional reversible work coarse-grained models with explicit electrostatics – an application to butylmethylimidazolium ionic liquids

Journal:	*Physical Chemistry Chemical Physics*
Manuscript ID	CP-ART-06-2018-003673
Article Type:	Paper
Date Submitted by the Author:	11-Jun-2018
Complete List of Authors:	Deichmann, Gregor; Technische Universitat Darmstadt, Chemistry van der Vegt, Nico; Technical University of Darmstadt, Center of Smart Interfaces

Article type: Full paper

Website www.rsc.org/pccp
Impact factor* 4.123

Journal expectations To be suitable for publication in *Physical Chemistry Chemical Physics* (*PCCP*) articles must include significant new insight into physical chemistry.

Article type: Full paper Original scientific work that has not been published previously. Full papers do not have a page limit and should be appropriate in length for scientific content.

Journal scope Visit the *PCCP* website for additional details of the journal scope and expectations.

PCCP is an international journal for the publication of cutting-edge original work in physical chemistry, chemical physics and biophysical chemistry. To be suitable for publication in *PCCP*, articles must include significant new insight into physical chemistry; this is the most important criterion that reviewers should judge against when evaluating submissions. Example topics within the journal's broad scope include:

- Spectroscopy
- Dynamics
- Kinetics
- Statistical mechanics
- Thermodynamics
- Electrochemistry
- Catalysis
- Surface science
- Quantum mechanics
- Theoretical research

Interdisciplinary research areas such as polymers and soft matter, materials, nanoscience, surfaces/interfaces, and biophysical chemistry are also welcomed if they demonstrate significant new insight into physical chemistry.

Reviewer responsibilities Visit the Reviewer responsibilities website for additional details of the reviewing policy and procedure for Royal of Society of Chemistry journals.

When preparing your report, please:

- Focus on the originality, importance, impact and reliability of the science. English language and grammatical errors do not need to be discussed in detail, except where it impedes scientific understanding.
- Use the journal scope and expectations to assess the manuscript's suitability for publication in *PCCP.*
- State clearly whether you think the article should be accepted or rejected and include details of how the science presented in the article corresponds to publication criteria.
- Inform the Editor if there is a conflict of interest, a significant part of the work you cannot review with confidence or if parts of the work have previously been published.

Thank you for evaluating this manuscript, your advice as a reviewer for *PCCP* is greatly appreciated.

Dr Katie Lim Executive Editor
Royal Society of Chemistry, UK

Professor Seong Keun Kim Editorial Board Chair
Seoul National University, South Korea

**2016 Journal Citation Reports®, (Thomson Reuters, 2017)*

Conditional reversible work coarse-grained models with explicit electrostatics - an application to butylmethylimidazolium ionic liquids

Gregor Deichmann and Nico F. A. van der Vegt

June 11, 2018

Parametrization of non-bonded interactions is the key challenge in the development of new coarse-grained (CG) models. The conditional reversible work (CRW) method is unique among the systematic coarse-graining methods since it requires only the simulation of two molecules in vacuo, making parametrizations of new models computationally inexpensive. This method has been applied successfully to apolar systems and has recently been extended for the parametrization of models with explicit electrostatics. In this work the ECRW is used to parametrize models for butylmethylimidazolium (BMIM) ionic liquids with three different cations. Results of subsequent CG simulations are used to illustrate the strengths and weaknesses of the resulting models. In particular, the structural and dynamical properties of the bulk, as well as the behavior at the vapor-liquid interface are studied. It is

shown that the ECRW coarse-graining method produces CG models of high quality for all selected test systems.

1 Introduction

Coarse-grained (CG) models are of great importance to the research of soft matter systems.[1,2] Molecular simulations in coarse resolution allow for the study of systems on time and length scales that are not accessible to atomistic models. In systematic coarse-graining methods a model is generated based on a finer (usually atomistic) representation of the system.[2] A variety of methods exist in the literature that are based either on structural correlations or on forces in the fine-grained (FG) system.[2–12]

The quality of a CG model can be judged using two aspects: representability and transferability. Representability describes the quality of a model in reproducing the system at a state point at which it was parametrized, while transferability describes the capability of a model to correctly reproduce the behavior of the system at different state points. Transferability can be introduced into a model by a variety of *a-posteriori* fits and additional model parameters (e.g. temperature-dependent interaction potentials).[9,13–19] Other approaches have focused more on the possibility to design the coarse-graining procedure such that the transferability of the model emerges as a natural consequence of the manner in which the interaction potentials are calculated.[3–5,20–23]

This idea is the basis of the conditional reversible work (CRW) method.[3] Here, the forces between two molecules in vacuo are used to exclude interfering multi-body correlations originating from the surrounding molecules, which are assumed to be among the leading causes of state-point dependence of CG models. While the original CRW method was developed for the parametrization of apolar systems, we recently published a modified version of the method. In this extended approach (which we shall refer to as ECRW in the following) we obtain separate effective interaction potentials for the Van-der-Waals and electrostatic components in the model.[4] We have shown in a model study that this

approach leads to a transferable CG force field for weakly polar molecular liquids. The purpose of this article is to demonstrate that the ECRW method is also suitable for the parametrization of force fields for components with a strong polar character. To this end, we parametrize force fields for three different butylmethylimidazolium ionic liquids (BMI-IL).

Room temperature ionic liquids (RTIL) have been of increasing interest in experimental research, as well as in molecular simulations.[24–29] Because of their high viscosity at room temperature, coarse-grained models are of great interest for the simulations of these systems. The long time scales required to equilibrate dense and viscous systems, such as IL, are more efficiently equilibrated using coarse-grained models.

The challenge of modeling RTIL in simulations lies in the correct description of the electrostatics of the system and several of methods and models have been brought forward that adress this challenge.[30] Since there are multiple coarse-grained models for BMI-IL in the literature,[31–35] the intent of this work is not merely to add to this variety. Rather we would like to point out a way to easily and efficiently parametrize CG models for ionic liquids or similar systems that can be applied in future applications, where a CG model for the system at hand may not be available. Since there is a clear physical significance to the interaction potentials obtained by parametrization with the ECRW method, it may be used to inexpensively compare mapping schemes and to gain insight into the interdependence of coarse-grained representation and model quality for a given system.

The remainder of this paper is structured as follows: In section 2 we shortly reiterate the essential steps of the ECRW method and introduce a novel technique of generating the trajectories required for the model parametrization. In section 3 the resulting models are presented. In sections 4 and 5 the parameters and results of subsequent simulations in the CG and FG representation are presented and discussed. Section 6 contains concluding remarks.

2 Methods

2.1 Extended conditional reversible work coarse-graining

We can obtain a coarse-grained model in a bottom-up manner using a fine-grained (i.e. atomistic) reference model and a mapping scheme that relates the fine-grained coordinates to the coarse-grained ones. In this work the mapping scheme is a center-of-mass mapping that defines the location of a CG site at the center of mass of topologically close atoms. Each fine-grained atom is part of exactly one CG site.

The parametrization of the CG model is performed using the extended (two-step) conditional reversible work (ECRW) method for polar systems. In the following a brief summary of the method will be given. For a detailed description we refer the reader to the existing literature.[4] In ECRW the pair interaction between CG sites i and j is modeled using effective Van-der-Waals and effective Electrostatic interactions ($A_{\mathrm{vdW}}(r_{ij})$ and $B_{\mathrm{ES}}(r_{ij})$). These interaction components are coupling free energies that correspond to the process of "switching-on" the respective interaction component for the atoms contained in the respective CG sites of interest, while these sites are constrained at distance r_{ij}. The interaction potential is calculated by means of a thermodynamic cycle using the reversible work W done against the intermolecular forces when two molecules approach from the cut-off distance to the finite distance r_{ij}. This reversible work can be calculated by integrating the constraint force F_{C}, i.e. the projection of the intermolecular force on the i-j distance vector:

$$F_{\mathrm{C}}(r_{ij}) = \left\langle \sum_{a\in\mathrm{Mol.1}} \sum_{b\in\mathrm{Mol.2}} \frac{\vec{F}_{ab}\cdot\vec{r}_{ij}}{|\vec{r}_{ij}|} \right\rangle \tag{1}$$

$$W(r_{ij}) = -\int_{r_{\mathrm{c}}}^{r_{ij}} F_{\mathrm{C}}(r')dr' \tag{2}$$

$$A_{\mathrm{vdW}} = W_{\mathrm{On,vdW}} - W_{\mathrm{Off}} \tag{3}$$

$$B_{\mathrm{ES}} = W_{\mathrm{On}} - W_{\mathrm{On,vdW}} \tag{4}$$

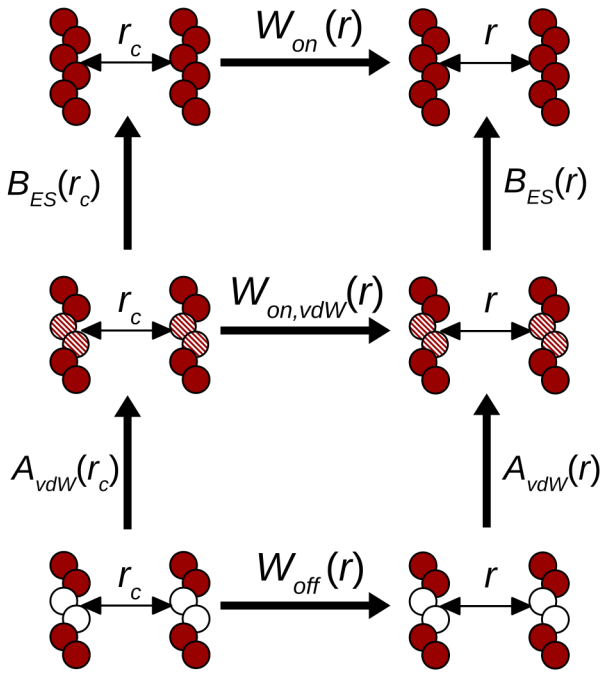

Figure 1: Schematic representation of the ECRW method. The CG interaction potentials A_{vdW} and B_{ES} represent the coupling free energy of "switching-on" the respective interaction components between the atoms included in a CG site. Here the two central atoms of a hexamer are merged into one CG site. The coupling free energies are calculated through thermodynamic cycles using the reversible work of moving the two sites of interest from quasi-infinite distance to the finite distance r.

The indices in the lowest two equations imply a procedure of turning on the Van-der-Waals component first and the electrostatic component second.

The energy components A_{vdW} and B_{ES} calculated in this manner are fitted using the functional forms introduced in reference[4]. For A_{vdW} the potential is approximated using a Morse-type potential with two stiffness parameters k_1 and k_2, controlling the stiffness

of the repulsive and attractive parts, respectively:

$$U_{\mathrm{vdW}}(r) = \varepsilon((1 - e^{-k_i(r-r_0)})^2 - 1) \begin{cases} i = 1 & \text{if } r \leq r_0 \\ i = 2 & \text{if } r > r_0 \end{cases}, \tag{5}$$

where ε is the potential well depth and r_0 is the minimum energy distance.

The electrostatic component is approximated using the Coulomb potential with the net charge q_i of the respective CG site i, calculated as the sum over all partial charges q_a of atoms a contained within the site:

$$q_i = \sum_{a \in i} q_a \tag{6}$$

$$U_{\mathrm{ES},ij}(r_{ij}) = \frac{1}{4\pi\varepsilon_0} \frac{q_i q_j}{r_{ij}} \tag{7}$$

2.2 Sampling of CRW trajectories

In past applications of the CRW method, the sampling of the constraint distance trajectories was performed by molecular dynamics simulations with a constraint algorithm ensuring a constant distance between beads of interest. In this work we use Monte-Carlo sampling to generate the trajectories used for the potential parametrization. The reason for this is that for systems with strong electrostatic interactions, such as the ionic liquids investigated here, we experienced sampling problems in constraint distance MD simulations. Since there are only two molecules in vacuo, highly attractive electrostatic energy between certain atoms can lead to conformations that are "trapped" in a local energy minimum. This hinders a sampling of the whole configuration space and therefore leads to very poor-quality potentials. Using Monte-Carlo moves, these local minima can be escaped thereby overcoming sampling issues. Also the simulations with the Monte Carlo approach tend to converge faster (with respect to the number of steps) than MD simulations performed in the past.

The Monte-Carlo algorithm employed here performs two kinds of trial moves:

1. Rotation of the whole molecule around the x-,y- or z-axis (one of which is randomly chosen)

2. Torsional rotation of a molecule around a randomly selected (σ)-bond

After each move the modified molecule is shifted such that the distance between the relevant CG sites is kept constant. The resulting conformation is accepted on basis of the Metropolis criterion:

$$p_{\text{accept}} = \begin{cases} 1 & \text{if } \Delta U \leq 0 \\ \exp\left(-\frac{\Delta U}{k_{\text{B}} T}\right) & \text{if } \Delta U > 0 \end{cases}, \tag{8}$$

where $\Delta U = U_{\text{new}} - U_{\text{old}}$ is the energy difference between the current and the previous configuration. T and k_{B} denote the temperature and Boltzmann constant, respectively. After accepting or rejecting the trial configuration, F_{C} is calculated from the current configuration.

With this Monte-Carlo simulation we can efficiently sample spatial orientations and torsional states of the molecules. Bond lengths and angles are kept constant in this approach, we assume their influence on the resulting potential to be negligible.

3 Parametrization of the coarse-grained model

3.1 Mapping scheme

In this work three different ionic liquid systems will be simulated: a butyl-methyl-imidazolium cation ($[\text{BMIM}]^+$) is combined with hexafluorophosphate ($[\text{PF}_6]^-$), tetrafluoroborate ($[\text{BF}_4]^-$) and chloride ($[\text{Cl}]^-$) anions. For $[\text{BMIM}]^+$and $[\text{PF}_6]^-$we use the all-atom force field published by Bhargava and Balasubramanian[36]. The interaction parameters of $[\text{BF}_4]^-$are taken from a different force field[32], while for $[\text{Cl}]^-$we use the

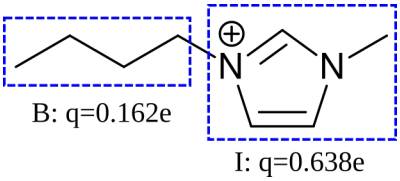

Figure 2: Mapping scheme employed for the coarse-graining of the BMIM cation including the net charges of sites B and I as calculated from the atomistic charges.

Lennard-Jones parameters of the OPLS-AA forcefield.[37] The cation and all anions have an absolute charge of 0.8 e.

Based on this atomistic representation of $[BMIM]^+[X]^-$ we define a center-of-mass mapping that maps the anions on one site and the cation on two sites. The cation is mapped such that the butyl and methylimidazolium units are contained within one CG site each (see fig. 2). These CG sites are named B (butyl) and I (methylimidazolium) respectively. Summing the atomistic charges yields a total net charges of 0.162 e and 0.638 e for the B and I sites respectively.

3.2 Interaction potentials

Using the Monte-Carlo algorithm described above, we perform simulations to generate interaction potentials for $[BMIM]^+[X]^-$. To this end, MC simulations of all CG site pairs in vacuo are performed at constant distances from 0.30 nm to 1.30 nm with a distance increment of 0.02 nm. The cutoff length for the Lennard-Jones potential is set to 1.3 nm, while electrostatic interactions are simulated using the Coulomb potential with infinite cutoff length. Single simulations have a length of 10^6 MC moves and the temperature is set to 500 K. Spatial and torsional rotation each make up for 50% of the trial moves. The maximum attempted rotation angle is 90 degrees for both molecular and torsional rotations. The overall acceptance rates are between 30% and 75% depending on the molecular distance. The force between the two molecules is written every 100 moves.

After integration of the molecular pair force, the potentials A_{vdW} and B_{ES} are obtained.

A_{vdW} is fitted using the equation 5. The resulting parameters are shown in table 1. B_{ES} is approximated using the Coulomb potential and the net charge of the respective coarse-grained bead resulting from the mapping scheme employed in the coarse-graining procedure (see Fig. 3 and 4 for a comparison for selected interaction pairs). From this comparison we conclude that the point charge assumption made in the CG model is justified for almost all interaction pairs. Relatively strong deviations however occur in all pairs containing the B site. This is likely due to the fact, that the charge of the butyl group contained in this site resides mostly on the α-carbon. This leads to a relatively large distance between center of mass and center of charge of this particular group of atoms and consequently the assumption of a point charge residing at the CG site's center of mass is less valid. However, the overall charge of the butyl group is the weakest in the model and the deviations are therefore small in an absolute reference frame.

In initial bulk simulations for $[\mathrm{BMIM}]^+[\mathrm{PF_6}]^-$at 500 K the liquid density was slightly overestimated. This mismatch is corrected for in a trial-and-error manner by slightly increasing the repulsive stiffness parameter k_1 of the potentials where the mismatch in the corresponding pair correlation function is the largest (I-I and I-$\mathrm{PF_6}$). Further, r_0 of the I-$\mathrm{PF_6}$ and I-$\mathrm{BF_4}$ interaction potentials is increased by 0.014 nm. For the $[\mathrm{BF_4}]^-$and $[\mathrm{Cl}]^-$systems, the anion-cation interaction is also slightly modified (to yield more repulsive potentials that lead to a better density reproduction). An overview of A_{vdW} and the potential used in the model is given in fig. 5 for all pairs, where such modifications have been performed. Using these modified potentials will lead to a more accurate reproduction of the density, without drastically changing the shape of the interaction potentials.

The intramolecular degree of freedom that is remaining within the $[\mathrm{BMIM}]^+$ion in the CG representation (i.e. the bond length between the B and I site) is parametrized using the Boltzmann inversion method. An MD trajectory of 100 ns is generated using one molecule in vacuo at 500 K, using a Langevin thermostat with a time constant

Table 1: Non-bonded parameters of the CG force field

	ε / kJ mol^{-1}	r_0 / nm	k_1 / nm^{-1}	k_2 / nm^{-1}	q / e
B-B	1.87	0.671	6.97	10.8	0.162
B-I	2.67	0.601	5.87	10.1	
I-I	2.90	0.573	10.3	7.98	0.638
B-PF_6	2.90	0.573	10.3	7.98	
I-PF_6	3.44	0.570	8.50	10.6	
PF_6-PF_6	3.16	0.571	12.3	11.4	-0.8
B-BF_4	1.98	0.531	10.7	7.56	
I-BF_4	2.68	0.538	9.30	10.7	
BF_4-BF_4	1.56	0.526	11.0	12.3	-0.8
B-Cl	2.18	0.447	15.0	7.96	
I-Cl	2.06	0.500	9.70	12.1	
Cl-Cl	1.23	0.378	18.5	12.7	-0.8

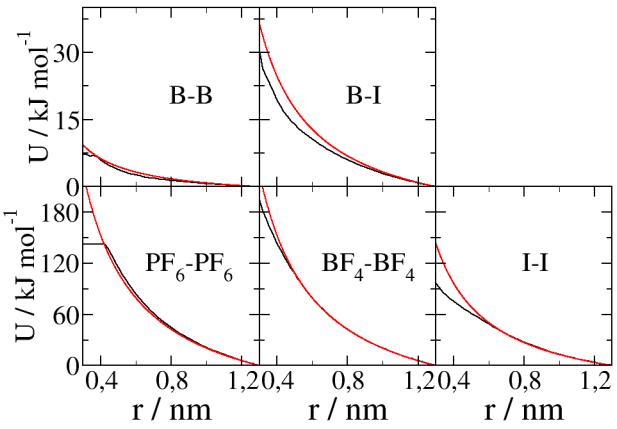

Figure 3: Comparison of the electrostatic component of the CRW potential B_{ES} (black) and the (shifted) Coulomb potential using the net charges of the CG sites (red) for all pairs with repulsive electrostatic interaction.

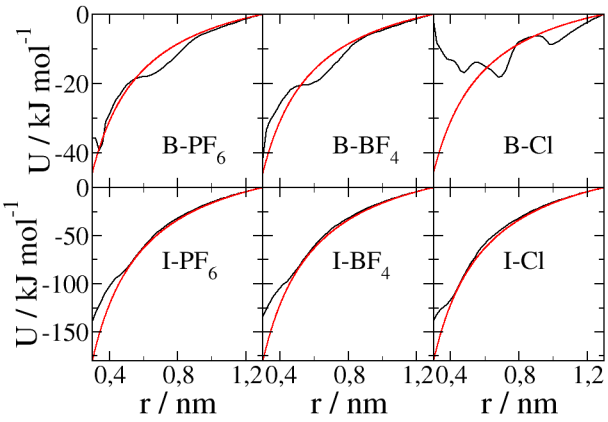

Figure 4: Comparison of the electrostatic component of the CRW potential B_{ES} (black) and the (shifted) Coulomb potential using the net charges of the CG sites (red) for all pairs with attractive electrostatic interaction.

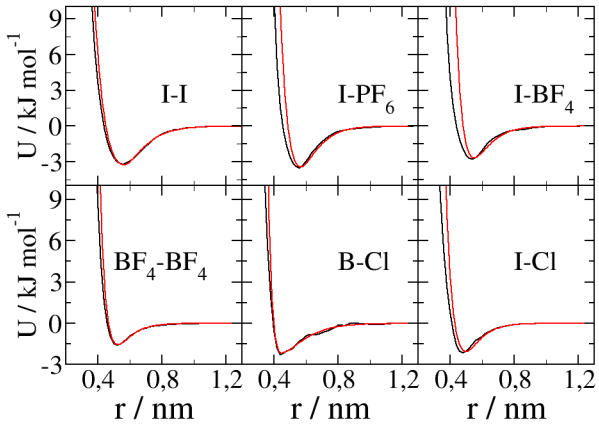

Figure 5: Comparison of the calculated CRW potential A_{vdW} (black) and the interaction potential used in the CG simulation (red) for all pairs, where modifications to the original fit have been performed.

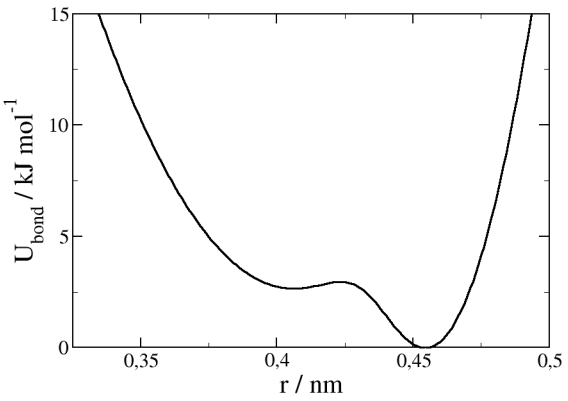

Figure 6: Bonded potential used to model the B-I bond.

of 1 ps. All nonbonded interactions between atoms are excluded from this simulation. The trajectory is mapped using the mapping scheme introduced above and the distance distribution $\rho(r)$ between the B and I sites is extracted from the mapped configurations. From this distribution the bonded interaction potential is calculated through:

$$U_{\mathrm{bond}}(r) = -k_{\mathrm{B}}T \ln\left(\frac{\rho(r)}{r^2}\right) + C, \tag{9}$$

where C is chosen such that $\min(U_{\mathrm{bond}}) = 0$. The resulting potential is shown in fig. 6.

4 Computational detail

For all systems, we conduct bulk MD simulations in an NPT-ensemble at 500 K and 1 bar. We generate 2 ns of trajectory starting from equilibrated initial structures using a time step of 1 fs. Cut-off distances are chosen at 1.3 nm. The Nose-Hoover thermostat[38] and Parrinello-Rahman barostat[39] are used with respective time constants of 1 and 5 ps. The atomistic simulations where conducted using Gromacs version 4.6.7[40], while the CG simulations where performed using LAMMPS.[41] The long-range part of the electrostatics is simulated using PME[42] (AA systems) and P3M[43] (CG systems). In the

Table 2: Resulting mass densities and vapor-liquid surface tensions

	ρ / kg m^{-3}		γ_{lv} / mN m^{-1}	
system	AA	CG	AA	CG
$[BMIM]^+[PF_6]^-$	1216	1221	28.5±7.5	28.0±0.3
$[BMIM]^+[BF_4]^-$	1035	1041	25.7±1.8	26.5±0.4
$[BMIM]^+[Cl]^-$	1011	1071	28.4±2.6	28.3±0.4

atomistic simulations long-range corrections for the Lennard-Jones potentials are applied to pressure and energy.

In addition to the NPT bulk simulations, NVT simulations are carried out with a half empty box to study the behavior of the liquid-vapor interface. To this end, the final configuration from the NPT simulation is taken and the box is extended by a factor of 2 in the z-direction. Simulations are performed using NVT molecular dynamics with identical settings as for the NPT bulk simulations described above and a simulation length of 50 ns.

5 Simulation results and discussion

5.1 Bulk structure and density

The mass density resulting from the NPT simulations are listed in table 2. From these results we observe that the densities from the CG simulation match the atomistic reference for $[BMIM]^+[PF_6]^-$and $[BMIM]^+[BF_4]^-$. This was intended by the modification of the potential parameters of the CG site pairs. On the other hand, the density of $[BMIM]^+[Cl]^-$is roughly 6 % higher in the CG model as compared to the atomistic model. In the parametrization we decided to keep a larger mismatch in the density with the aim of not skewing interaction potentials too much in comparison to the potentials resulting from the CRW calculations.

Figures 7-9 show the radial distribution functions $g(r)$ for all systems in the atomistic

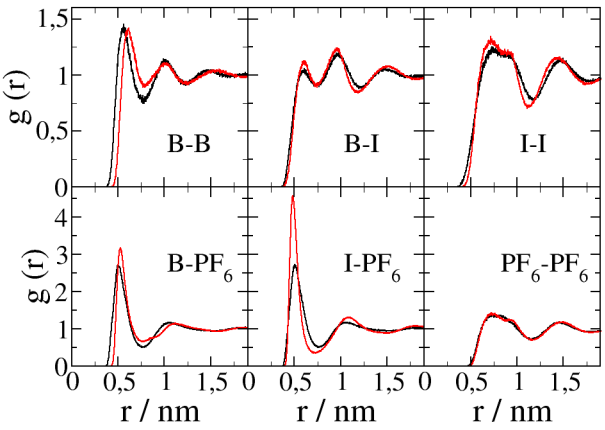

Figure 7: Radial distribution functions of all site pairs of $[BMIM]^+[PF_6]^-$as calculated from the atomistic (black) and coarse-grained (red) simulations.

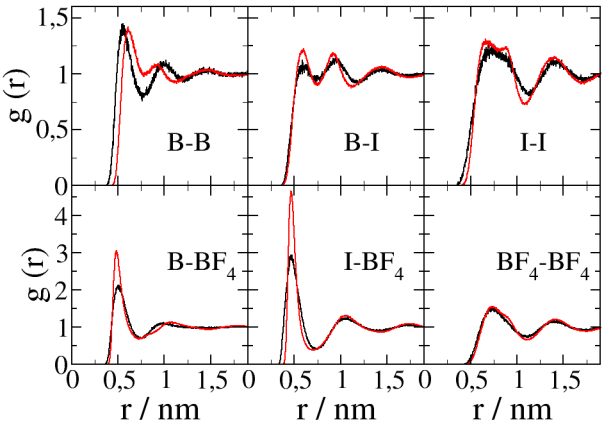

Figure 8: Radial distribution functions of all site pairs of $[BMIM]^+[BF_4]^-$as calculated from the atomistic (black) and coarse-grained (red) simulations.

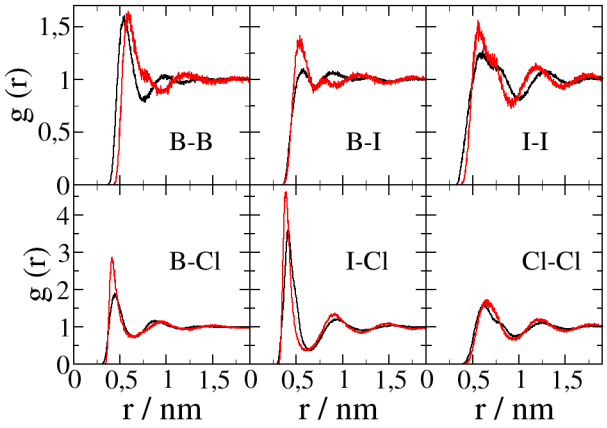

Figure 9: Radial distribution functions of all site pairs of $[BMIM]^+[Cl]^-$as calculated from the atomistic (black) and coarse-grained (red) simulations.

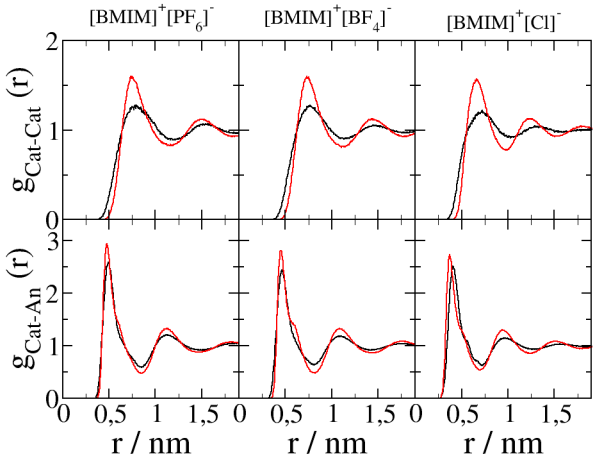

Figure 10: Radial distribution functions of the molecular centers of mass. Distributions of Cation-Cation pairs and Cation-Anion pairs for all systems are shown in the upper and lower half, respectively, for the atomistic (black) and CG systems (red).

and CG representation.

For $[BMIM]^+[PF_6]^-$the structure is well reproduced (see fig. 7). The CG model is capable to reproduce the $g(r)$ for the pairs I-I, B-I, and PF_6-PF_6 almost quantitatively. For the remaining pairs, we can observe small deviations with respect to the excluded volumes (larger for B-B and B-PF_6) which is probably due to the mapping of an almost linear chain on a spherical CG site and the resulting underestimation of orientation effects Further, the first peak in the $g(r)$ of I-PF_6 is much higher in the CG simulation than in the atomistic reference. We attribute this to the fact that the charge of the I bead is localized in one point in the CG model as opposed to the charge distribution over multiple atoms in the atomistic model. An analogous argument can be made for the B-PF_6 RDF, which suffers from a similar mismatch.

For $[BMIM]^+[BF_4]^-$similar conclusions can be drawn (see fig. 8). The reproduction of the $g(r)$ is good by standards of other CRW models. However, it is less accurate than the reproduction for the system containing $[PF_6]^-$. Notable effects in the $[PF_6]^-$system are also observed here (increased excluded volume for B-B and increased first peak for I-BF_4).

The CG model for $[BMIM]^+[Cl]^-$(see fig. 9) does not perform to the same degree as the two other models. The $g(r)$ is only reproduced to quantitative extent for the Cl-Cl pair, the potential of which is identical in the CG and atomistic models. For other pairs a qualitative reproduction of characteristic features is achieved. Most notably, the $g(r)$ of the B-I pair considerably deviates from the atomistic reference. This mismatch is probably caused by the treatment of the electrostatic interactions in the CG model. Figure 4 shows that the deviation from Coulomb-like point charge behavior is largest for the B-Cl site pair. The overestimation of attractive electrostatic forces is countered, to a certain degree, by the modification of the effective Van-der-Waals interactions, but still we might assume that the balance between the site-site interactions is somewhat ill-represented in the resulting CG model. The fact that the $[Cl]^-$ion is the smallest

among the studied anions adds to this effect, since for this system the electrostatic forces are stronger as in the other systems.

A comparison of the RDFs of the molecular centers of mass for cations and anions (fig. 10) gives a further interesting insight into the differences in the molecular structure between the two models. In these RDFs a mismatch in the cation-cation distribution is observed: the first peak of these distributions is higher and narrower for all systems studied. This is especially interesting, since none of the site-site RDFs (Figures 7-9) shows a comparably large mismatch. On the other hand, the cation-anion RDFs are far better reproduced, despite larger mismatches in the RDFs of the single CG site pairs. For the anion-anion RDFs (see figures 7-9) the distributions calculated from CG simulations reproduce the atomistic reference. The reason for this mismatch of the molecular pair correlations is probably the treatment of the electrostatic in the coarse-grained model. While the assumption of a point charge at the center of mass is a fair assumption for the highly rigid and spherically symmetric anions, it is a very coarse approximation of the cation, which is more flexible and has a smeared out distribution of the charge within the molecule. The cation in the CG representation will necessarily be more rigid in terms of the charge distribution, and this fact reflects in more pronounced minima and maxima in the cation-cation RDF.

5.2 Dynamic properties and speed-up rates

The self-diffusion coefficient D of any molecule can be calculated from the slope of the mean squared displacement $\langle \Delta x^2 \rangle$ using the Einstein relation:

$$D = \lim_{t \to \infty} \frac{1}{6t} \left\langle \Delta x^2(t) \right\rangle \tag{10}$$

In addition we calculate the ionic conductivity λ of the ionic liquids using the following

Table 3: Self-diffusion coefficients of all investigated systems

System		D / cm^2 s^{-1} AA	CG	Speed-up	λ / S m^{-1} AA	CG	Speed-up
$[BMIM]^+[PF_6]^-$	Cation	1.05	1.17	1.11	27.5	35.7	1.3
	Anion	0.65	1.24	1.91			
$[BMIM]^+[BF_4]^-$	Cation	1.24	1.55	1.25	96.6	102	1.1
	Anion	1.23	1.74	1.41			
$[BMIM]^+[Cl]^-$	Cation	0.55	1.74	3.16	50.2	104	2.1
	Anion	0.74	2.31	3.12			

Green-Kubo relation:[44]

$$\lambda = \frac{1}{3Vk_{\mathrm{B}}T}\int_0^\infty \left\langle \vec{J}(t)\cdot\vec{J}(0)\right\rangle dt, \tag{11}$$

where $\vec{J} = e\sum_{i=0}^{n_{\mathrm{ion}}} z_i\vec{v}_i$ is the current calculated from the ions' respective velocities and charges.

The self-diffusion coefficients and ionic conductivities calculated from the trajectories of the liquid system are listed in table 3.

In general, the diffusion coefficients are higher in the CG system. An acceleration of dynamics is common in systematically coarse-grained models. It is linked to the softer potential energy surface of the CG model in comparison to the fine-grained representation. The rate is different for all investigated systems and also differs between anions and cations.

The speed-up rates of the diffusion coefficient are small for the models with $[PF_6]^-$and $[BF_4]^-$anions and larger for the system with the $[Cl]^-$anion. This finding correlates with the quality of reproduction of the liquid structure. For the investigation of dynamical quantities it is especially the heterogeneous speed-up for the two different molecules in the system that one has to be aware of since mechanisms of dynamic phenomena may be qualitatively changed by the difference in relative diffusion speed.

A similar trend is observed for the ionic conductivity: the speed-up is small for the sys-

tems with $[PF_6]^-$and $[BF_4]^-$, whereas for the $[Cl]^-$system a larger speed-up is observed. A comparison to experimental data is not undertaken here, because the atomistic models used for the reference simulations strongly vary in their quality of reproduction of the experimental data.

5.3 Properties of the liquid-vapor interface

From the simulations of the liquid-vapor interface we can calculate the liquid-vapor surface tension γ_{lv} using the well-established relation:

$$\gamma_{\mathrm{lv}} = \frac{L_{\mathrm{z}}}{2}\left\langle p_{\mathrm{zz}} - \frac{p_{\mathrm{xx}} - p_{\mathrm{yy}}}{2}\right\rangle, \tag{12}$$

where L_{z} is the length of the box parallel to the interface normal vector (in this case the z-axis) and p_{ii} denotes the diagonal elements of the stress tensor. Table 2 shows that the values for γ_{lv} calculated from CG simulations match the atomistic reference values for all within error bars. This result shows that CRW-based potentials for the ionic liquid systems are transferable to liquid-vapor interfaces, a result that has been observed for other CRW CG models.[3,4,45]

In addition to the γ_{lv}, we use the results from the liquid-vapor interface simulation to analyze the density profile along the interface for all systems. The densities of the respective anion and cation molecules are shown in fig. 11. Much like in the case of the liquid structure, we can observe that the CG models of $[BMIM]^+[PF_6]^-$and $[BMIM]^+[BF_4]^-$reproduce the atomistic density distribution of both the cation and anion well with only small deviations. For the $[BMIM]^+[Cl]^-$the deviations of the CG simulations with respect to the atomistic system are larger, as might be expected from the deviations observed for the bulk density. Still the CG model is capable of a qualitative reproduction of the density profile for both ion types.

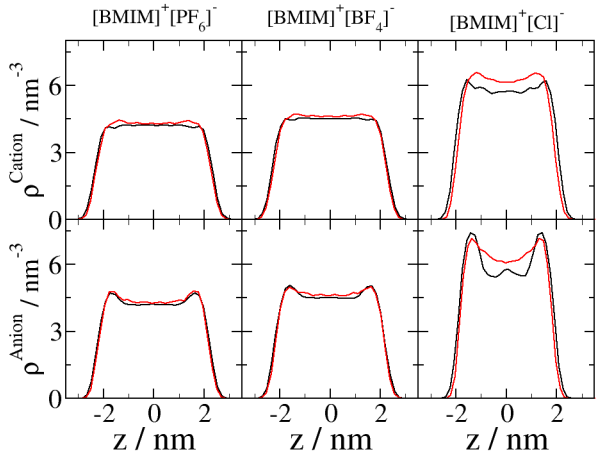

Figure 11: Molecular number density along the z-axis of a half empty box for all ionic liquids. We compare the atomistic reference (black) to the CG simulation results (red) for $[BMIM]^+$(upper half) and the respective anion (lower half).

6 Conclusions

In this article, an attempt has been presented to apply the extended conditional reversible work introduced in an earlier publication[4] to systems of ionic liquids. To this end, we have parametrized CG models for the $[BMIM]^+$cation in combination with $[PF_6]^-$,$[BF_4]^-$, and $[Cl]^-$anions. After small modifications that serve to slightly enhance the repulsive character of the interaction potentials but do not change the general shape or the attractive part, models have been obtained with effective Van-der-Waals and electrostatic components. These ECRW models are capable of reproducing the liquid bulk density and liquid structure of $[BMIM]^+[PF_6]^-$and $[BMIM]^+[BF_4]^-$, while for $[BMIM]^+[Cl]^-$the model is less predictive.

The reason for the larger disagreement of the $[BMIM]^+[Cl]^-$CG model with respect to the liquid structure is probably in the chemical nature of the system itself. In contrast to the $[PF_6]^-$and $[BF_4]^-$ions, the charge of the $[Cl]^-$ion is not spread over multiple atoms. This makes the assumption of Coulomb-type electrostatic interactions for the CG force field less accurate.

The self-diffusion coefficients have been studied and we can observe an acceleration of the diffusional dynamics in all studied systems. Here again the $[BMIM]^+[Cl]^-$systems stands out. The speed-up for this system is larger, while in the other two systems the diffusion coefficients are increased by a lesser degree.

In addition, the liquid-vapor surface tension has been calculated for the three IL systems. Here we find that for all three systems γ_{lv} is quantitatively reproduced within error bars. This finding is in accordance with the results obtained for other systems modeled with CRW-based potentials[3,4,45] and illustrates the state-point transferability of these models. A reliable reproduction of the vapor-liquid interface is important especially in the context of modeling wetting phenomena. We demonstrate here a method by which CG models of molecules with ionic character can be parametrized in a straightforward and computationally cheap manner from an existing atomistic force field.

We would like to point out again that the aim of this article is not merely the publication of another CG model for imidazolium ionic liquids. Rather, we intend to demonstrate that the ECRW method is suitable for the parametrization not just of weakly polar molecules but also for systems that have a stronger ionic character. It has been shown that this is indeed possible and that the resulting potentials may well be used to simulate vapor-liquid interfaces of ionic liquids.

Supporting Information

An implementation of the Monte-Carlo sampling algorithm used for the parametrization of the ECRW potentials shown in this work will be available for download at www.github.com/GDeichmann.

Acknowledgement

Financial support for this work was granted by the Deutsche Forschungsgemeinschaft (DFG) through the Collaborative Research Center Transregio TRR 146 Multiscale Simulation Methods for Soft Matter Systems.

References

[1] C. Peter and K. Kremer, *Faraday Discussions*, 2010, **144**, 9.

[2] E. Brini, E. A. Algaer, P. Ganguly, C. Li, F. Rodríguez-Ropero and N. F. A. van der Vegt, *Soft Matter*, 2013, **9**, 2108.

[3] E. Brini, V. Marcon and N. F. A. van der Vegt, *Physical Chemistry Chemical Physics*, 2011, **13**, 10468.

[4] G. Deichmann and N. F. A. van der Vegt, *Journal of Chemical Theory and Computation*, 2017, **13**, 6158–6166.

[5] Y. Wang, W. G. Noid, P. Liu and G. A. Voth, *Physical Chemistry Chemical Physics*, 2009, **11**, 2002.

[6] W. G. Noid, J.-W. Chu, G. S. Ayton, V. Krishna, S. Izvekov, G. A. Voth, A. Das and H. C. Andersen, *The Journal of Chemical Physics*, 2008, **128**, 244114.

[7] D. Reith, M. Pütz and F. Müller-Plathe, *Journal of Computational Chemistry*, 2003, **24**, 1624–1636.

[8] A. Lyubartsev and A. Laaksonen, *Physical Review E*, 1995, **52**, 3730–3737.

[9] P. Ganguly, D. Mukherji, C. Junghans and N. F. A. van der Vegt, *Journal of Chemical Theory and Computation*, 2012, **8**, 1802–1807.

[10] M. S. Shell, *The Journal of Chemical Physics*, 2008, **129**, 144108.

[11] J. W. Mullinax and W. G. Noid, *The Journal of Physical Chemistry C*, 2010, **114**, 5661–5674.

[12] J. McCarty, A. J. Clark, J. Copperman and M. G. Guenza, *The Journal of Chemical Physics*, 2014, **140**, 204913.

[13] J. W. Mullinax and W. G. Noid, *The Journal of Chemical Physics*, 2009, **131**, 104110.

[14] F. Cao and H. Sun, *Journal of Chemical Theory and Computation*, 2015, **11**, 4760–4769.

[15] H.-J. Qian, P. Carbone, X. Chen, H. A. Karimi-Varzaneh, C. C. Liew and F. Müller-Plathe, *Macromolecules*, 2008, **41**, 9919–9929.

[16] B. M. Mognetti, L. Yelash, P. Virnau, W. Paul, K. Binder, M. Müller and L. G. MacDowell, *The Journal of Chemical Physics*, 2008, **128**, 104501.

[17] B. M. Mognetti, P. Virnau, L. Yelash, W. Paul, K. Binder, M. Müller and L. G. MacDowell, *The Journal of Chemical Physics*, 2009, **130**, 044101.

[18] B. Hess, C. Holm and N. van der Vegt, *The Journal of Chemical Physics*, 2006, **124**, 164509.

[19] A. Villa, C. Peter and N. F. A. van der Vegt, *Journal of Chemical Theory and Computation*, 2010, **6**, 2434–2444.

[20] T. Sanyal and M. S. Shell, *The Journal of Chemical Physics*, 2016, **145**, 034109.

[21] T. Sanyal and M. S. Shell, *The Journal of Physical Chemistry B*, 2018, **122**, 5678–5693.

[22] V. Krishna, W. G. Noid and G. A. Voth, *The Journal of Chemical Physics*, 2009, **131**, 024103.

[23] T. T. Foley, M. S. Shell and W. G. Noid, *The Journal of Chemical Physics*, 2015, **143**, 243104.

[24] H. Weingärtner, *Angewandte Chemie International Edition*, 2008, **47**, 654–670.

[25] Y. Wang, W. Jiang, T. Yan and G. A. Voth, *Accounts of Chemical Research*, 2007, **40**, 1193–1199.

[26] F. Dommert, K. Wendler, R. Berger, L. Delle Site and C. Holm, *ChemPhysChem*, 2012, **13**, 1625–1637.

[27] M. Salanne, *Physical Chemistry Chemical Physics*, 2015, **17**, 14270–14279.

[28] E. J. Maginn, *Accounts of Chemical Research*, 2007, **40**, 1200–1207.

[29] Q. R. Sheridan, W. F. Schneider and E. J. Maginn, *Chemical Reviews*, 2018, **118**, 5242–5260.

[30] E. J. Maginn, *Journal of Physics: Condensed Matter*, 2009, **21**, 373101.

[31] J. Zeman, F. Uhlig, J. Smiatek and C. Holm, *Journal of Physics: Condensed Matter*, 2017, **29**, 504004.

[32] C. Merlet, M. Salanne and B. Rotenberg, *The Journal of Physical Chemistry C*, 2012, **116**, 7687–7693.

[33] Y. Wang, S. Feng and G. A. Voth, *Journal of Chemical Theory and Computation*, 2009, **5**, 1091–1098.

[34] Y. Wang, S. Izvekov, T. Yan and G. A. Voth, *The Journal of Physical Chemistry B*, 2006, **110**, 3564–3575.

[35] D. Roy and M. Maroncelli, *The Journal of Physical Chemistry B*, 2010, **114**, 12629–12631.

[36] B. L. Bhargava and S. Balasubramanian, *The Journal of Chemical Physics*, 2007, **127**, 114510.

[37] W. L. Jorgensen and P. Schyman, *Journal of chemical theory and computation*, 2012, **8**, 3895–3801.

[38] S. Nosé, *Molecular Physics*, 1984, **52**, 255–268.

[39] M. Parrinello and A. Rahman, *Journal of Applied Physics*, 1981, **52**, 7182–7190.

[40] B. Hess, C. Kutzner, D. van der Spoel and E. Lindahl, *Journal of Chemical Theory and Computation*, 2008, **4**, 435–447.

[41] S. Plimpton, *Journal of Computational Physics*, 1995, **117**, 1–19.

[42] T. Darden, D. York and L. Pedersen, *The Journal of Chemical Physics*, 1993, **98**, 10089–10092.

[43] R. W. Hockney and J. W. Eastwood, *Computer simulation using particles.*, A. Hilger, Philadelphia, 1988.

[44] J.-P. Hansen and I. R. McDonald, *Theory of simple liquids*, Elsevier / Academic Press, Amsterdam ; Boston, 3rd edn., 2007.

[45] E. Brini and N. F. A. van der Vegt, *The Journal of Chemical Physics*, 2012, **137**, 154113.